Arsenic migration to deep groundwater in Bangladesh influenced by adsorption and water demand

K.A. Radloff, Y. Zheng, H.A. Michael, M. Stute, B. C. Bostick, I. Mihajlov, M. Bounds, M. R. Huq, I. Choudhury, M.W. Rahman, P. Schlosser, K. M. Ahmed, A. van Geen

Supplementary Methods

Batch adsorption experiments

The batch adsorption experiments were conducted on freshly collected drill cuttings and groundwater and were prepared in the field under near anaerobic conditions within a few hours of collection in a nitrogen-filled portable glove box (Bel-Art). Groundwater was collected from a nearby well (Table S1) and kept anoxic. Brown sediments were collected by traditional manual well drilling at 55 m and 58 m depth, and gray sediments at 40 m and 46 m depth (Table S2). In the batch isotherm (BI) experiment, Langmuir adsorption isotherms were constructed from As additions ranging from 440 to 32,000 μg L^{-1} and sampled after 145 hours (Table S3). Kinetic parameters were determined on sediment from 40 and 58 m by monitoring a 3,000 μg L^{-1} addition of As(III) over 400 hours, referred to as the batch kinetic (BK) experiments (Table S4). Groundwater As concentrations were altered in the batch experiments using an 1,000 mg L^{-1} As spike prepared from reagent grade $NaAsO_2$ or $NaHAsO_4 \cdot 7H_2O$.

As adsorption push-pull tests

Each push-pull test, one for As(III) and one for As(V), required a receiving well and the same source well was used for both tests. All wells were screened at ~ 60 m in the deep aquifer zone and had a similar geochemical composition (Table S1). The source well was pumped with a locally available irrigation pump at 12 L min^{-1}, while a high-pressure gradient piston pump

(Cole-Parmer) was used to introduce the concentrated As and Br solution at 2 mL min^{-1} into the source water. Approximately 1,000 litres of low-As groundwater was dynamically modified to contain ~200 μg L^{-1} of As(III) or As(V) and ~50 mg L^{-1} Br. This mixture was immediately injected into the receiving well to limit the geochemical alteration of the groundwater. An inflation packer (Solinst) was deployed at 45 m to limit dilution. For As(V), 1240 L of groundwater with 190 μg L^{-1} of As(V) and 40.0 mg L^{-1} of Br was injected into a well 9 m from the source well (Table S5). For As(III), 780 L of groundwater with 210 μg L^{-1} of As(III) and 55.5 mg L^{-1} of Br was injected into a well 11 m from the source well (Table S6). Adsorption was monitored through 21 pulls of 100 L over 9 days.

Bromide only push-pull test

Two separate wells, screened at 65 m and 10 m apart, at the same location were used for a Br only push-pull test. During this experiment, 540 L of deep groundwater dynamically mixed with Br and injected into the receiving well with a Br concentration of 130 mg L^{-1}. This injection was followed by 80 L of groundwater without tracer, to enhance dispersion. The tracer solution was allowed to rest in the aquifer for 2 days and then 907 L of groundwater was pumped out at one time (Table S7).

Field Measurements

Groundwater was continuously monitored for temperature, pH and conductivity using a multi-parameter water monitoring probe in a flow cell (MP 556 from YSI, Inc.). Dissolved oxygen (Chemetrics) and alkalinity were measured using standard methods [1], with As(III) and As(V) separation by a sorption-based cartridge [2].

Laboratory Analyses

Groundwater samples acidified to 1% HCl (Optima) were analyzed by High-Resolution Inductively Coupled Plasma Mass Spectrometry (HR ICP-MS) for As, Fe, Mn, S and P [3]. Supernatant from batch experiments were filtered through 0.45 μm syringe filters before HR ICP-MS analysis, with As(III) determined using differential pulse cathodic stripping voltammetry (DPCSV) [4,5]. Bromide was measured by ion chromatography (IC) [6].

Coarse fraction (sand) analysis separated the sediment into three size fractions: >150 μm, 63-150 μm, and <63 μm [7]. The porosity of the aquifer was assumed to be 0.25 with a bulk density of 2.65 g cm^{-3} based on the BGS characterization of the deeper aquifer [8]. Sediment from the batch isotherms underwent a sequential extraction to remove sorbed As using distilled water (24 hr), 1M phosphate (24 hr) and 1.2 N HCl (60 °C for 24 hrs). The samples from the extractions were then analyzed for As using an ICP-MS (Thermo, Waltham, MA) operating in the automated Collision Cell Technique (CCT) model [9]. Mn minerals were also measured in sediments that received either no or the largest As addition with x-ray absorption near edge spectroscopy (XANES) using standard methods [10].

Adsorption equations

The adsorption of As to sediment surface can be described using the Langmuir model as follows:

$$\frac{dS}{dt} = \frac{\theta}{\rho} k_f C (1 - \frac{S}{S_{max}}) - k_r S \qquad \text{(eq. 1)}$$

where C is the dissolved concentration [μg L^{-1}], S is the sorbed concentration [μg kg^{-1}], S_{max} is the sorption capacity [μg kg^{-1}], θ is the porosity [L L^{-1}], ρ is the bulk density [kg L^{-1}], k_f

is the adsorption rate constant [hr^{-1}] and k_r is the desorption rate constant [hr^{-1}] [11]. At equilibrium, equation 1 becomes:

$$K = \frac{\theta}{\rho} * \frac{k_f}{k_r} = \frac{S}{C * (1 - \frac{S}{S_{max}})} \qquad \text{(eq. 2)}$$

K [L groundwater kg^{-1} sediment] can be understood as similar to the partitioning coefficient K_d (defined as the ratio of sorbed As (S) to dissolved As (C)), but includes the adsorption capacity (S_{max}). At low concentrations when S $\ll$ S_{max}, K_d is nearly identical to K.

The heterogeneity of sediment surfaces was treated as though one site was present, but that adsorption occurs first on the readily available, rapidly adsorbing sites (the "fast" sites) following eq. 1, and is then transferred by diffusion to the less available, "slow" adsorbing sites[12], thus there are two-steps of adsorption. Equation 1 was modified to include the transfer of sorbed As from the fast to the slow sites, represented by a simple diffusion reaction, thus the sorption on the fast sites can be described as:

$$\frac{dS_f}{dt} = \frac{\theta}{\rho} k_f C (1 - \frac{S_f}{S_{max}}) - k_r S_f + \frac{k_{diff} * (S_s - S_f)}{x_f} \qquad \text{(eq. 3)}$$

where S_f is the sorbed concentration on the fast sites [µg kg^{-1}], S_s is the sorbed concentration on the slow sites [µg kg^{-1}], x_f is the fraction of fast to total sites [dimensionless], and k_{diff} is the rate of exchange from the fast to the slow sites [hr^{-1}]. The model assumes there is no difference in the sorption capacity (S_{max}) or equilibrium partitioning (K) between the two site types, so at equilibrium $S_f = S_s$. The As concentration on the slow sites is described as:

$$\frac{dS_s}{dt} = \frac{k_{diff} * (S_f - S_s)}{1 - x_f}$$
(eq. 4)

Model for push-pull experiments

A simple model was constructed to implement the sorption reactions described in equations 3 and 4 during the injection (push) and extraction (pull) phases of the experiments. Common analytical approaches [13,14] to modelling such tests were not possible since the pull was conducted step-wise, with brief periods of pumping for sampling followed by gradually longer intervals of rest. This model tracks the concentrations of dissolved As and sorbed As on fast and slow sites in discrete, equal volume rings surrounding the well. The concentric rings were composed of 100 L of groundwater and 795 kg of sediment, assuming a sediment density of 2.65 g cm^{-1} and a porosity of 0.25 [8]. The model assumes homogenous plug flow with no dispersion or additional advection in the aquifer and therefore, only samples with little mixing, as indicated by [Br]/ [Br]$_0$ >0.85, were used for model fitting. Since injection was rapid (approximately 3 hrs), the rings were filled within minutes during the push phase. However, the time between "pulls" is large (from 1 to 24 hours), so the resting time was divided into 20 equal-sized time steps to have sufficiently small dt in eqs. 3 and 4 to account for reaction in each ring. The one-step model was evaluated using x_f=1. The best fit of parameters were achieved by minimizing the least square differences between the modelled concentrations and the measured total dissolved As concentration for the undiluted samples used for model. The first sampling point was ignored because the concentrations are changing so rapidly that small timing differences at this point significantly altered the fit of the other data. The sensitivity of model results to the box size was tested using a model with 10-fold smaller boxes (each box with 10 L of groundwater) and this did not substantially change results.

Groundwater Flow and Solute Transport Model

The 3D groundwater model was modified from the flow-only model of Michael and Voss [15-17] to include advective-dispersive transport. This added complexity enables simulation of solute concentrations, which are the values measured in groundwater and relevant for human health. Model geometry, shown in Figure S1, and flow boundary conditions (steady-state, prescribed head at the elevation of the land surface across the top of the model) are described in Michael and Voss [15,16]. Transport boundary conditions are $C=1$ in the top 1 m of the aquifer within the high-As area (Fig. S5) and $C=0$ in the top 1 m elsewhere. Initial concentration is $C_0=1$ within the top 50 m of the high-As area, $C_0=0$ elsewhere (Fig. S1), which is consistent with observations of As concentrations with depth, *e.g.* BGS and DPHE [8]. Sorption is modelled at depths below 94 m over most of the basin (in some areas, where permeable sediments are thin, this zone becomes shallower) with retardation factors of 1, 14.2, and 133.5. This is equivalent to equilibrium K_d values of 0 (no adsorption), 1.2, and 12 L kg^{-1} assuming a porosity of 0.2 [16] and a solid density of 2.65 g cm^{-3} (that is, quartz). The K_d of 1.2 L kg^{-1} is the average of the most conservative estimates of As(III) and As(V) adsorption from the push pull experiments, while the K_d of 12 L kg^{-1} is simply an order of magnitude greater. Longitudinal dispersivity was set to 100 m, consistent with literature values on the scale of vertical arsenic transport (150-200 m) [18, 19], horizontal transverse dispersivity was 0.1 m, and vertical transverse dispersivity was 0.01 m.

Supplementary Results

This section provides a comprehensive summary of additional data and experimental results that were used to assess As adsorption on the brown sediments as well as the flow and transport model of the Bengal Basin. The experimental site location and geochemical characteristics of the aquifer are described first. A summary of the adsorption experimental results is given next. This is followed by description of the flow and transport model and parameters used.

Characteristics of Groundwater and Sediment

The site of the sorption and push-pull experiments (90.6° E, 23.8° N), located 30 km east of Dhaka, has been described previously [20]. The deeper, brown aquifer has low concentrations of As, P, S, Mn and Fe, a near neutral pH and an alkalinity of approximately 8 mEq L^{-1} (Table S1). Groundwater chemistry was similar in the four wells screened between 55 and 59 m used in the brown adsorption experiments. Shallow groundwater from the gray sediments was obtained from a depth of 41 m and had a similar pH and sulphate content as the deeper groundwater. Groundwater As, Fe and P were higher, while groundwater Mn, alkalinity and conductivity were significantly lower.

The amount of As adsorbed or associated with amorphous Fe oxides on the sediment was assessed by sequential extraction. On the brown sediment, little As could be removed by desorption in distilled water, while 0.3 mg kg^{-1} was desorbed by 1M phosphate and an additional 0.8 mg kg^{-1} was removed with a warm, 1.2N HCl extraction (Table S2). Extractable As was greater and more variable in the gray sediment, with total extractable As ranging from 3.5 to 6.2 mg kg^{-1}. The drill cuttings are biased towards the larger grain sizes, as some of the clay and silt

particles are removed in the drilling process [21]. Grain size analysis of the cuttings indicated that they consisted of 87% sand, 11% silt and 2% clay by weight (Table S2), while core samples of a brown aquifer at nearby site showed a grain size distribution of 80% sand, 13% silt and 8% clay [22]. The cuttings from each depth had similar amounts of HCl-extractable Fe (10.7 and 10.8 g kg^{-1}, respectively). Again, the composition of the gray sediments were more variable, but were predominately sand and the HCl-extractable Fe ranged from 7.6 to 17.8 g kg^{-1}.

X-ray absorption near edge spectroscopy (XANES) was used identify Mn minerals present in the sediment. Most Mn was found in Mn^{2+} and Mn^{3+} minerals and little to no Mn^{4+} minerals were present (Figure S2).

The disperstivity of the aquifer was estimated by fitting the results of the bromide only push-pull test using the analytical solution proposed by Schroth *et al.*[13]. The initial low Br concentrations in the pull were due to the injection of an additional 80 L of groundwater without tracer, such a situation cannot be addressed with the analytical method and therefore the fit of the Br data from these early time points were not considered. The aquifer is assumed to have a porosity of 0.25 [8] and the radius of influence was calculated to be 73 cm. Best fit, determined by least squares, was achieved with a disperstivity of 0.5 cm (Figure S3). Over 90% of the injected Br was recovered when the volume removed during the pull equalled the volume injected (V=V$_0$) and 97% was recovered by the end of the experiment when V= 1.5 V$_0$.

Adsorption Experiments: Estimating K

Batch isotherm (BI) experiments determined equilibrium partitioning (K) and capacity (S$_{max}$) for As(III) and As(V) in both brown and gray sediments (Table S3). Batch kinetic (BK)

experiment monitored As(III) adsorption kinetics over 400 hours (Table S4). Push-pull tests evaluated As(III) and As(V) adsorption *in situ* over 200 hours (Tables S5 and S6).

The BI experiments show that As(III) and As(V) adsorption onto brown sediment are non-linear and can be approximated by Langmuir isotherms (Figure 2). At environmentally relevant concentrations when solute [As] is < 3,000 μg L^{-1} (Table S3), over 90% of As were found to be adsorbed by the sediment. The amount of As adsorbed on the sediment was calculated from the loss in groundwater, while the initial adsorbed As was assumed to be negligible. The isotherm experiments were assumed to be at or near equilibrium. Using the Langmuir isotherm (eq. 1), K and S_{max} were determined to be 20 L kg^{-1} and 40,000 μg As kg^{-1} sediment, respectively, for both As(III) and As(V). Higher estimates of K were obtained when considering only samples spiked with <3,000 μg L^{-1} of As (29 and 49 L kg^{-1} for the As(III) and As(V) additions, respectively, Table S3). The K of the batch kinetic (BK) experiment was determined to be 68 L kg^{-1} for As(III) at 400 hours (Table S4). The slow kinetics of As adsorption likely resulted in the observed range of Ks in the batch experiment, as equilibrium may not have been reached in the BI experiments and this effect would be more pronounced with larger additions.

The batch experiments on shallow, gray sediment demonstrated a lower partitioning than observed in the brown sediments (Figure 2 and S4). Since saturation was not reached in these experiments, As adsorption can only be described using the partition coefficient, K_d. The K_d is approximately 1.5 L kg^{-1} in the three BI experiments, with no difference observed between As(III) and As(V). At 40 m, the K_d is 1.4±0.1 L kg^{-1} (r^2=0.95) and 1.6±0.1 L kg^{-1} (r^2=0.98) for As(III) and As(V), respectively, while at 46 m the K_d for As(III) is 1.1±0.1 L kg^{-1} (r^2=0.99).

Adsorption was more rapid in the gray sediment than the brown, with near complete adsorption by 5 hrs and a K_d of 1.1 ± 0.2 L kg^{-1} (excluding the sample from 64 hrs, Table S4).

In the batch kinetic and push-pull experiments on brown sediments, As adsorption over time followed two- step kinetics, initially fast followed by a slower approach to equilibrium (Figure 1 and S5) [23-26]. The two-step kinetics of As adsorption may result from the slow diffusion to the interior surface sites that are less accessible. Groundwater As concentrations in the BK experiment of As(III) declined rapidly in the first 5 hours, and then at a slower rate between 5 and 400 hrs and was well described using the two-step model with 23% of the total As adsorption sites as readily available ("fast") sites (x_f) and 77% as slow sites (Figure S5). This proportion of fast sites is similar to other heterogeneous flood plain aquifers where interior space was estimated to comprise 70 to 90% of the total space available and was attributed to the presence of fine material, weathering and sand compaction [27-29]. Initially rapid and then slower As adsorption was also observed in the push-pull tests for As(III) and As(V) (Figure 1 and S6A). For the As(V) push-pull, 7 samples collected over 70 hours were relatively unaffected by dilution, defined as [Br]/[Br]$_0$ >0.85 (Table S5). As(V) was quickly adsorbed such that 80% of the injected [As(V)] (188 µg L^{-1}) was adsorbed in 6 hours, reaching a plateau of 90% (or 18 µg L^{-1}) by 45 hours. For the As(III) push-pull, 5 undiluted samples were collected over 48 hours (Table S6).   As(III) adsorption was slower compared to As(V), with only 60% of injected [As(III)] (213 µg L^{-1}) to have been adsorbed in the first 6 hours, about 80% by 50 hrs and a plateau of 90% was reached at 145 hours once considerable dilution had occurred. In both tests, the loss of As was much faster than would have occurred from dilution alone. Dilution occurred more quickly in the As(III) experiment because less groundwater was injected than in the As(V) experiment. The dilution within the experiments was similar; when the volume removed by the

pull equalled the amount injected ($V=V_0$) the Br recovery was 75 and 76% for As(V) and As(III), respectively.

Parameter estimation in the push-pull experiments rely on the estimation of the equilibrium partitioning, [K, L kg^{-1}], capacity [S_{max}, µg kg^{-1}], adsorption (forward) reaction rate constant, [k_f, hr^{-1}], the fraction of fast to total sites [x_f, dimensionless] and the diffusion rate constant between the two types of sites [k_{diff}, hr^{-1}] and the equations used are included in the Supplementary Methods. The same groundwater [As] can be simulated, however, with multiple combinations of K and x_f values.   Therefore, three different adsorption scenarios were considered (Figure 1 and Table S8). This process cannot identify a unique K for the aquifer sediments, but instead offers a plausible range of potential K values.

First, the conservative assumption that all adsorption sites are equal and readily accessible was used (one-step model, x_f= 100%) and this predicted the lowest K values (0.5 and 1.8 L kg^{-1} for As(III) and As(V), respectively, Table S8 and Figure 1).   The modelled groundwater As concentrations, however, plateau too early and does not reflect concentrations observed in the later, diluted points.   Second, the proportion of fast and slow sites (25 and 75%, respectively) from the batch kinetic experiment was used as an upper bound estimate of the availability of fast sites. This results in K's of 1.7 (r^2=0.96) and 5.1 (r^2=0.98) L kg^{-1} for As(III) and As(V), respectively.   Third, the K value for As(V) determined in the batch isotherm experiment, 50 L kg^{-1}, was used to fit the other parameters (k_f, x_f and k_{diff}) for the As(V) push-pull test. The proportion of fast sites was estimated to be only 3% of the total adsorption sites. The x_f and k_{diff} from the As(V) experiment was then used to estimate K and k_f for As(III) since these factors are measures of the aquifer properties; best fits was achieved with a K value about 4-fold smaller (13 L kg^{-1}) and k_f value 2-fold slower than As(V) adsorption. In all models S_{max}

was set at 40,000 µg kg^{-1}, based on the batch isotherm experiments. The calculated diffusion rate is sufficiently slow that little As is transferred to the slow sites during the push phase (<5%), but during the pull phase As is steadily diffusing and becomes equally distributed in the two phases. It is also important to note the non-linear sensitivity of K to determination of fast adsorbing sites.

These results give a plausible range of adsorption that may be achieved and also illustrates that potential importance of both intra- and intergranular pore spaces in adsorption. The batch kinetic experiment estimated that 77% of adsorption sites were slower to adsorb. While we did not investigate the mechanisms controlling the difference in adsorption rates, one common explanation is intragranular porosity. In a similar sandy, quartz-based aquifer on Cape Cod, intragranular porosity was estimated to be 80% [27]. If the majority of the fast sites are located on the surface (while most slower sites are intragranular), it is obvious that access to many of the fast sites will become restricted in the compacted aquifer to the intergranular spaces, as compared to essentially infinite intergranular spaces for a well shaken slurry. Access to fast sites may also be restricted by transport of As along larger preferential flow paths during the rapid injection of the push, where groundwater penetrated over 1 m into the aquifer in 3 hours, while vertical recharge is estimated to be on the order of centimetres to meters per year in Bangladesh [30,31]. Should the injection of high-As water be slower, the modelled interior sites might become more comparable to the estimates of intragranualar porosity. Adsorption in the push-pull tests likely falls between the 2 estimates of fast sites (3% and 25% of all sites). The batch results should be considered a high-end estimate and may not be representative of the adsorption that will occur in the actual aquifer. As the kinetic analysis demonstrates, As adsorption on brown sediment is not instantaneous, but equilibrium is reached on the order of

days to weeks and this rate is rapid relative to the rate of natural groundwater flow. Therefore under natural flow conditions As adsorption should not be limited by kinetics and a larger partitioning could be expected.

Kinetic limitations, and therefore partitioning as low as 0.5 L kg^{-1}, may still be important in cases of well failure (where there is breakage of the pipe or flow along the casing). The rates of vertical groundwater flow in these scenarios are not known, but are presumably much faster. In Araihazar, the hydraulic head of deeper aquifer is typically 50 cm to 1 m lower than the shallow aquifer [22], thus considerable amounts of water could flow through a broken well casing. These point sources of As contamination could be a large source of As into the deeper aquifer and deserves further attention.

Adsorption Experiments: Further considerations

Arsenic speciation of the groundwater was measured in the batch isotherms and push-pull tests to assess potential differences in sorption of As species and to determine if significant oxidation or reduction was occurring. It has been suggested that only As(V) is effectively adsorbed on the brown sediment and As(III) adsorption is the result of its oxidization by Mn^{4+} oxides in the sediment and then adsorption as As(V) [32]. The isotherms for As(III) and As(V) at 58 m are very similar and there was no significant oxidation of the As(III) additions (Figure S7) suggesting no difference in sorption by As species. The voltammetry measurements are based on standard additions and require a high level of dilution, which also increases the error associated with these measurements. The samples for which the percent of As(III) is greater than 100% are regarded as containing only As(III), since the total As concentration is considered the more accurate measure of concentration. In the As(V) push-pull test, minor amounts (between 3 and 7 μg L^{-1}) of As(III) were detected using the Meng columns and were not considered to be

significant (Table S5).   The As(III) injection had 13% As(V) during the injection phase and varied between 15 and 28% in the undiluted samples, however there was no trend over time (Table S6). It is unclear if there was indeed 13% As(V) in the injection solution, which seems unlikely, or if this ratio reflects a limitation of the columns' use in the field. Regardless, the lack of a trend in percent of As(III) do not support the idea of extensive As(III) oxidation. Insignificant amounts of Mn^{4+} oxides were identified using XANES and no other reactive minerals were found that would induce As oxidization on the sediment (Figure S2). These results suggest that while it is clear that As(III) adsorption is slower and can be significantly limited on shorter time scales, this does not result from the need for extensive As(III) oxidation or the lack of As(III) adsorption capacity on the sediment.

A variety of water parameters were measured during the push-pull experiments, even though the experiments were designed to minimize any differences between the source and receiving wells. In general there was good agreement between the dissolved constituents of the two wells (Table S1). The three properties that could have the largest influence on As chemistry are the dissolved oxygen, [Fe] and [P]. Low levels of dissolved oxygen were detectable in all wells, but were not correlated with [Fe] and [P] (Figure S6). In both experiments, [P] decreased from 0.6 to 0.4 mg L^{-1} reflecting the slight difference between the source and receiving wells. In the As(III) experiment the initial loss of P was slightly greater than would have been expected from mixing alone, but by later time points there was no net change in groundwater P. The injected groundwater [Fe] was lower than either receiving well and remained low, between 0.1 and 0.4 mg L^{-1}, during the experiment. Groundwater [Mn] reflected the slight differences between the receiving wells and, similar to the [P], there was initially a slight loss in Mn in the As(III) experiment, but this was not sustained over time. The pH was slightly higher in the

source well (7.3) than in the receiving wells (6.8) and pH decreased from 7.2 to about 7.0 over the course of the experiment and remained slightly elevated from what was expected based on mixing alone.

Adsorption is assumed to be reversible in the Langmuir isotherm and this was confirmed by the sequential extraction of sediments from the batch experiments (Table S3). Water alone was unable to remove much adsorbed As in 24 hrs suggesting that the kinetics of desorption are much slower than adsorption, as is commonly observed[11]. The following two steps (1M phosphate and warm, 1.2 N HCl) recovered 90 to 130% of the As adsorbed during the batch experiments. Most of the recovered As was removed in the phosphate extraction. A similar proportion, and not absolute amount, of As was then extracted by HCl regardless of size of the spike.

Groundwater Flow and Solute Transport Model

Simulations were run with three pumping scenarios, as described in the main text: split scheme ('S', irrigation pumping 50-100 m depth, domestic pumping 150-200 m depth) and deep scheme ('D', both domestic and irrigation pumping 150-200 m depth), with two domestic pumping rates for the split scheme, 50 L person^{-1} day^{-1} ('SC', estimated current rate, also used in the deep scheme) and 200 L person^{-1} day^{-1} ('SH', possible future rate with increased population and usage). K_d values of 0, 1.2, and 12 were simulated for each of the three pumping scenarios and are referred to as SC0, SC1, SC10 and so forth. Simulation results are shown in Figure 3 and S8. Though sorption provides some protection to the deep parts of the aquifer system, the deep pumping rate strongly affects the vulnerability of deep resources.

Additional simulations were run to assess the influence of vertical hydraulic conductivity on As breakthrough. The model base case [15] was a Kh:Kv of 10,000:1 in the split scenario with current pumping rates and a K_d of 1.2 L kg^{-1} (SC1) and additional runs increased the vertical conductivity, by decreasing the anisotropy to 1,000:1 and 100:1 for the SCI scenario; results are also shown in Table S9.

References

1   Gran, G. A new method to linearize titration curves. *Analyst* **77** (1952).

2   Meng, X. G., Korfiatis, G. P., Jing, C. Y. & Christodoulatos, C. Redox transformations of arsenic and iron in water treatment sludge during aging and TCLP extraction. *Environmental Science & Technology* **35**, 3476-3481 (2001).

3   Cheng, Z., Zheng, Y., Mortlock, R. & van Geen, A. Rapid multi-element analysis of groundwater by high-resolution inductively coupled plasma mass spectrometry. *Analytical and Bioanalytical Chemistry* **379**, 512-518 (2004).

4   He, Y., Zheng, Y., Ramnaraine, M. & Locke, D. C. Differential pulse cathodic stripping voltammetric speciation of trace level inorganic arsenic compounds in natural water samples. *Analytica Chimica Acta* **511**, 55-61 (2004).

5   Jung, H. B. & Zheng, Y. Enhanced recovery of arsenite sorbed onto synthetic oxides by L-ascorbic acid addition to phosphate solution: calibrating a sequential leaching method for the speciation analysis of arsenic in natural samples. *Water Research* **40**, 2168-2180 (2006).

6   USEPA.   Method 300: Determination of Inorganic Anions by Ion Chromatography (eds Environmental Monitoring Systems Laboratory, Office of Research and Development, Cincinnati, OH, 1993).

7   Poppe, L. J., Hastings, P. & Polloni, C. USGS East Coast Sediment Analysis: Procedures, Database and Georeferenced Displays. *U.S. Geological Survey Open-File Report 00-358* (2000).

8   BGS/DPHE (British Geological Survey, Dept. of Public Health Engineering, Bangladesh). *Arsenic Contamination of Groundwater in Bangladesh, Final Report* (Keyworth, UK, 2001).

9   He, Y. & Zheng, Y. Assessment of in vivo bioaccessibility of arsenic in dietary rice by a mass balance approach. *Science of the Total Environment* **408**, 1430-1436, doi:10.1016/j.scitotenv.2009.12.043 (2010).

10   Quicksall, A. N., Bostick, B. C. & Sampson, M. L. Linking organic matter deposition and iron mineral transformations to groundwater arsenic levels in the Mekong delta, Cambodia. *Applied Geochemistry* **23**, 3088-3098, doi:10.1016/j.apgeochem.2008.06.027 (2008).

11   Limousin, G. *et al.* Sorption isotherms: A review on physical bases, modeling and measurement. *Applied Geochemistry* **22**, 249-275 (2007).

12   Wu, S. C. & Gschwend, P. M. Sorption Kinetics of Hydrophobic Organic- Compounds to Natural Sediments and Soils. *Environmental Science & Technology* **20**, 717-725 (1986).

13   Schroth, M. H., Istok, J. D. & Haggerty, R. In situ evaluation of solute retardation using single-well push-pull tests. *Advances in Water Resources* **24**, 105-117 (2001).

14   Cassiani, G., Burbery, L. F. & Giustiniani, M. A note on in situ estimates of sorption using push-pull tests. *Water Resources Research* **41**, W03005 (2005).

15   Michael, H. A. & Voss, C. I. Controls on groundwater flow in the Bengal Basin of India and Bangladesh: regional modeling analysis. *Hydrogeology Journal* **17**, 1561-1577, doi:10.1007/s10040-008-0429-4 (2009).

16   Michael, H. A. & Voss, C. I. Estimation of regional-scale groundwater flow properties in the Bengal Basin of India and Bangladesh. *Hydrogeology Journal* **17**, 1329-1346, doi:10.1007/s10040-009-0443-1 (2009).

17   Michael, H. A. & Voss, C. I. Controls on groundwater flow in the Bengal Basin of India and Bangladesh: regional modeling analysis. *Hydrogeology Journal* **17**, 1561-1577, doi:10.1007/s10040-008-0429-4 (2009).

18   Gelhar, L. W.,Welty, C. & Rehfeldt, K. R. A critical review of data on field-scale dispersion in aquifers. *Water Resources Research* **28**, 1955-1974 (1992).

19   Neuman, S. P. Universal scaling of hydraulic conductivities and dispersivities in geologic media. *Water Resources Research* **26**, 1749-1758 (1990).

20   Radloff, K. A. *et al.* Mobilization of arsenic during one-year incubations of gray aquifer sands from Araihazar, Bangladesh. *Environmental Science & Technology* **41**, 3639-3645 (2007).

21   Horneman, A. *et al.* Decoupling of As and Fe release to Bangladesh groundwater under reducing conditions. Part I: Evidence from sediment profiles. *Geochimica et Cosmochimica Acta* **68**, 3459-3473 (2004).

22   Zheng, Y. *et al.* Geochemical and hydrogeological contrasts between shallow and deeper aquifers in two villages of Araihazar, Bangladesh: Implications for deeper aquifers as drinking water sources. *Geochimica et Cosmochimica Acta* **69**, 5203-5218 (2005).

23   Fuller, C. C., Davis, J. A. & Waychunas, G. A. Surface-chemistry of Ferrihydrite. 2. Kinetics of arsenate adsorption and coprecipitation. *Geochimica et Cosmochimica Acta* **57**, 2271-2282 (1993).

24   Raven, K. P., Jain, A. & Loeppert, R. H. Arsenite and arsenate adsorption on ferrihydrite:

Kinetics, equilibrium, and adsorption envelopes. *Environmental Science & Technology* **32**, 344-349 (1998).

25   Selim, H. M. & Zhang, H. Arsenic adsorption in soils: Second-order and multireaction models. *Soil Science* **172**, 444-458 (2007).

26   Wu, S. C. & Gschwend, P. M. Sorption Kinetics of Hydrophobic Organic- Compounds to Natural Sediments and Soils. *Environmental Science & Technology* **20**, 717-725 (1986).

27   Wood, W. W., Kraemer, T. F. & Hearn, P. P. Intragranular diffusion - An important mechanism influencing solute transport in clastic aquifers. *Science* **247**, 1569-1572 (1990).

28   Harvey, C. F. & Gorelick, S. M. Rate-limited mass transfer or macrodispersion: Which dominates plume evolution at the Macrodispersion Experiment (MADE) site? *Water Resources Research* **36**, 637-650 (2000).

29   Haggerty, R. & Gorelick, S. M. Multiple-rate mass-transfer for modeling diffusion and surface-reactions in media with pore-scale heterogeneity. *Water Resources Research* **31**, 2383-2400 (1995).

30   Harvey, C. F. *et al.* Arsenic mobility and groundwater extraction in Bangladesh. *Science* **298**, 1602-1606 (2002).

31   Stute, M. *et al.* Hydrological control of As concentrations in Bangladesh groundwater. *Water Resources Research* **43** (2007).

32   Stollenwerk, K. G. *et al.* Arsenic attenuation by oxidized aquifer sediments in Bangladesh. *Science of the Total Environment* **379**, 133-150 (2007).

Supporting Tables

S1   Groundwater characteristics

S2   Sediment characteristics

S3   Batch isotherm experimental data

S4   Batch kinetic experimental data

S5   Push-pull data from the As(V) injection

S6   Push-pull data from the As(III) injection

S7   Push-pull data from the Br only injection

S8   Results of the As adsorption experiments

S9   Model results for one observation location and high-As area at approximately 160 m depth

Supporting Figures

S1   Model geometry, finite difference grid, and boundary and initial conditions for solute transport

S2   Mn speciation by X-ray absorption near edge spectroscopy (XANES)

S3   Br recovery over continuous pull with estimated disperstivity

S4   Batch isotherm results

S5   Batch kinetic results

S6   Groundwater constituents in the push-pull tests

S7   Speciation in the batch isotherms

S8   Areas of the deep low-As aquifer zones at risk of contamination, including simulations using K_d = 12 kg L^{-1}.

Table S1. Groundwater characteristics. The groundwater for the batch experiments was collected from I-1 for the brown sediments and I-2 for the gray sediments. The source water for both push-pull experiments came from I-4, while the receiving (rec.) wells were I-7 and I-9 for As(V) and As(III), respectively.

Well ID		I-1	I-4	I-7	I-9	I-2
Use		**Batch**	**Source**	**Rec. AsV**	**Rec. AsIII**	**Gray Batch**
Depth	m	55.9	59.7	57.9	58.5	41.1
pH		7.36	7.21	6.59	6.96	6.90
As	μg/L	2	2	1	2	210
AsIII	μg/L	2	2	1	1	200
P	mg/L	0.57	0.58	0.41	0.42	1.51
S	mg/L	0.05	0.09	0.33	0.07	0.14
Mn	μg/L	138	152	201	53	36
Fe	mg/L	0.40	0.59	0.53	0.15	3.31
Alkalinity	mEq/L	8.96	7.72	7.90	8.31	1.93
	+/-	0.21	0.31	0.28	0.32	0.05
Conductivity	mS/cm	1.18	0.92	1.13	1.20	0.07

Table S2. Sediment characteristics. Arsenic and Fe concentrations from the extraction of the sediment (drill cuttings) used in the batch experiments are shown as well as the relative grain sizes.

	Gray		Brown	
Extractions (mg/kg)	**40m**	**46m**	**55m**	**58m**
Water- ext As	0.03	0.39	0.00	0.00
Phosphate-ext As	1.10	1.92	0.37	0.28
HCl- ext As	2.37	3.86	0.68	0.88
Total Ext. As	3.50	6.17	1.05	1.16
Total Ext. Fe	17,790	7,580	10,650	10,820
Grain Size (% by weight)				
>150 μm	72.8	84.5	82.5	90.6
63-150 μm	20.5	7.7	14.2	7.8
<63 μm	6.7	7.8	3.3	1.6

Table S3. Batch isotherm experimental data. Compilation of the data collected for each bottle of the batch isotherm experiments, including total [As] and [As(III)], as well as the results from the desorption experiments. Samples from 55 and 58 m depth are brown sands, while the 40 and 46 m depth are gray sands from the high-As aquifer zone. Groundwater had 2.2 µg/L of As before additions to the brown sediments and 221 µg/L of As for the gray sediments. Dry weight was estimated for samples used in mineralogy analysis. Samples that were not analyzed are indicated with a 'na', while those with non-detectable concentrations are indicated by 'nd'.

Experiment	No.	GW	Sed.	pH	Dissolved As Initial	Dissolved As at 145 hrs	Speciation AsIII	Speciation % AsIII	Ads. As at 145 hrs	Extractions Water	Extractions Phos.	Extractions HCl	Extractions Total
		mL	g		µg/L	µg/L	µg/L		µg/kg	µg/kg	µg/kg	µg/kg	µg/kg
55m -AsIII	0	9.6	5.4	7.30	2	3	2	61%	-1	3	368	677	1,048
	1	9.6	5.4	7.31	445	37	26	70%	724	10	1,107	999	2,116
	3	9.6	5.3	7.34	888	44	nd		1,520	18	1,690	1,323	3,030
	5	9.6	5.5	7.31	1,773	306	643	210%	2,543	32	2,715	1,661	4,409
	7	9.6	5.0	7.30	3,544	619	198	32%	5,589	Sample for mineralogy			
58m -AsIII	0	9.6	4.7	7.31	2	1	nd		2	3	283	876	1,163
	1	9.6	5.6	7.40	445	38	69	182%	696	120	760	913	1,794
	2	9.6	4.8	7.33	666	18	nd		1,306	8	1,510	1,062	2,580
	3	9.6	4.7	7.34	888	34	nd		1,751	17	1,993	1,161	3,171
	4	9.6	5.3	7.39	1,330	76	121	159%	2,272	12	2,345	1,215	3,573
	5	9.6	5.6	7.40	1,773	141	236	167%	2,786	23	2,852	1,552	4,427
	6	9.6	5.6	7.37	2,658	163	141	87%	4,257	57	4,117	1,725	5,898
	7	9.6	7.2	7.47	3,544	318	368	116%	4,299	149	3,212	1,914	5,275
	8	9.6	5.3	na	7,086	728	na		11,548	453	10,012	3,358	13,822
	9	9.6	5.5	na	14,169	3,012	na		19,541	330	20,018	6,485	26,833
	10	9.6	5.0	na	28,336	10,306	na		34,847	Sample for mineralogy			
58m -AsV	1	9.6	3.9	7.40	502	22	na		1,179	16	1,624	1,028	2,668
	3	9.6	4.2	na	1,002	47	na		2,177	24	2,540	1,193	3,756
	5	9.6	4.7	7.36	2,002	89	na		3,878	27	3,901	1,420	5,348
	7	9.6	4.8	na	4,002	429	na		7,206	96	7,171	2,371	9,638
	8	9.6	5.4	na	8,002	1,158	na		12,169	90	11,198	3,505	14,793
	9	9.6	5.1	na	16,002	4,142	na		22,299	1,809	22,355	6,798	30,963
	10	9.6	5.0	na	32,002	12,641	na		37,079	Sample for mineralogy			
40m -AsIII	0	10	5.0	7.10	221	169	222	132%	105	26	1,096	2,374	3,496
	1	10	4.5	7.19	646	356	602	169%	644	4	2,190	2,412	4,606
	2	9.8	5.3	7.16	872	508	692	136%	671	33	2,249	2,945	5,227
	3	9.6	5.4	7.18	1,107	570	1,060	186%	957	26	1,916	2,523	4,466
	4	9.6	5.1	7.11	1,549	877	1,170	133%	1,266	193	1,751	3,334	5,278
	5	9.6	5.9	7.14	1,992	1,086	1,470	135%	1,480	65	1,870	2,309	4,245
	6	9.6	4.7	7.16	2,877	1,480	2,140	145%	2,833	179	4,158	3,565	7,903
	7	9.6	6.8	7.18	3,763	2,298	3,010	131%	2,617	Sample for mineralogy			
40m -AsV	1	9.6	5.3	7.21	721	461	456	99%	473	24	1,953	2,448	4,426
	4	9.6	5.6	6.93	1,721	820	1,410	172%	1,532	281	1,743	3,259	5,284
	5	9.6	4.5	6.67	2,221	1,391	2,600	187%	1,759	20	2,402	4,115	6,537
	7	9.6	4.3	7.20	4,221	2,361	4,070	172%	4,178	4	5,810	4,847	10,661
46m -AsIII	0	9.6	5.3	7.22	221	211	370	176%	19	387	1,917	3,862	6,166
	1	9.6	4.9	7.24	664	467	na		383	155	2,223	4,379	6,757
	3	9.6	4.3	7.24	1,107	714	863	121%	877	570	2,425	4,617	7,611
	5	9.6	5.5	7.28	1,992	1,192	na		1,388	458	2,113	3,988	6,559
	7	9.6	6.8	7.33	3,763	2,241	2,930	131%	2,546	Sample for mineralogy			

23

Table S4. Batch kinetic experimental data. As adsorption was monitored over 400 hrs. The experiment on brown sediments used 34.5 g (dry) sediment collected from drill cuttings at 58 m and 150 mL of groundwater from well I-1, while 49.2 g of gray sediments were collected at 40 m and 140 mL of groundwater from well I-2.

Time	Brown Sediment		Gray Sediment	
	Dissolved As	Adsorbed As	Dissolved As	Adsorbed As
hr	µg/L	µg/kg	µg/L	µg/kg
0	2,893	0	3,226	0
5	2,256	2,713	2,249	2,811
10	1,657	5,263	2,162	3,061
28	1,271	6,907	2,299	2,667
40	932	8,355	2,476	2,156
64	659	9,514	1,191	5,855
400	232	11,336	2,375	2,447

Table S5. Push-pull data from the As(V) injection. Compilation of the data collected during the As(V) push-pull experiment, which used water from well I-4, modified it with 190 µg/L of As and pushed it into well I-7. The pH and DO measurements and the As(III) column separation were conducted in the field, while samples for the other parameters were measured in the lab. The double line indicates when significant dilution began ($[Br]/[Br]_0 < 85\%$) and 'na' indicates samples that were not analyzed.

Sample	Time	Vol.	Br	As	AsIII	As III	P	S	Mn	Fe	DO kit	Alk.		pH
	hr	L	mg/L	µg/L	µg/L	%	mg/L	mg/L	µg/L	mg/L	ppm	meq/L	+/-	
Receiving well				2	2		0.41	0.33	201	0.53		7.90	0.28	6.59
Source well				1	1		0.58	0.09	152	0.59		7.72	0.31	7.21
Injection	3.0	1,240	40	189	0	0%	0.59	0.11	129	0.23	0.15	9.04	0.78	7.25
1	1.5	101	40	80	7	9%	0.58	0.08	167	0.36	0.25	8.95	1.37	7.25
2	3.5	204	39	56	6	11%	0.58	0.12	159	0.39	0.40			7.20
3	6.3	302	40	38	5	13%	0.56	0.10	152	0.16	0.25			7.35
4	12.4	399	37	32	6	20%	0.56	0.15	158	0.16	0.20			7.28
5	24.1	505	36	27	5	17%	0.55	0.19	158	0.21	0.20			6.96
6	44.5	607	37	18	4	22%	0.53	0.22	146	0.16	0.15	7.37	0.08	7.18
7	68.8	697	36	20	4	22%	0.54	0.24	157	0.27	0.15			7.07
8	92.8	783	32	17	3	18%	0.51	0.16	161	0.35	0.25			7.17
9	116.5	872	22	16	3	20%	0.55	0.20	159	0.26	0.15			7.04
10	142.0	961	17	13	4	30%	0.52	0.21	162	0.29	0.06			6.71
11	166.3	1,049	17	na	na	na	na	na	na	na	0.10			7.01
12	189.0	1,136	6	12	4	31%	0.51	0.32	185	0.33	0.40			7.24
13	213.9	1,236	4	11	4	34%	0.47	0.27	173	0.26	0.20			6.80
14	214.8	1,354	2	8	3	37%	0.50	0.27	159	0.21	0.10			
15	215.5	1,440	1	8	2	27%	0.43	0.21	139	0.16	0.20			7.01
16	216.2	1,536	na	na	na	na	na	na	na	na	0.30			
17	217.0	1,634	na	na	na	na	na	na	na	na	0.20			7.01
18	217.8	1,737	na	7	na	na	0.43	0.17	120	0.15	0.40			
19	218.8	1,836	na	na	na	na	na	na	na	na	0.15			6.89
20	219.8	1,942	na	na	na	na	na	na	na	na	0.15			6.88
21	220.3	2,045	na	6	2	37%	0.40	0.14	112	0.11	0.10			6.90

Table S6. Push-pull data from the As(III) injection. Compilation of the data collected during the As(III) push-pull experiment, which used water from well I-4, modified it with 215 µg/L of As and pushed it into well I-9. The pH and DO measurements and the As(III) column separation were conducted in the field, while samples for the other parameters were measured in the lab. The double line indicates when significant dilution began ($[Br]/[Br]_0 < 85\%$) and 'na' indicates samples that were not analyzed.

Sample	Time	Vol.	Br	As	AsIII	As III	P	S	Mn	Fe	DO kit	Alk.		pH
	hr	L	mg/L	µg/L	µg/L	%	mg/L	mg/L	µg/L	mg/L	ppm	meq/L	+/-	
Receiving well				2	1		0.42	0.07	53	0.15		6.90	0.22	6.78
Source well				1	1		0.58	0.09	152	0.59		7.72	0.31	7.21
Injection	2.6	783	56	213	186	87%	0.57	0.07	120	0.20	0.02	7.35	0.28	7.19
1	1.9	112	58	127	105	83%	0.54	0.07	94	0.15	0.60	7.76	0.14	7.00
2	4.1	215	56	112	94	84%	0.58	0.06	83	0.08	0.40			7.22
3	6.0	313	54	88	74	85%	0.53	0.07	79	0.54	0.40			7.19
4	23.8	429	57	66	48	72%	0.49	0.06	67	0.07		7.00	0.33	7.13
5	47.6	548	48	49	35	72%	0.50	0.11	64	0.09	0.70			7.15
6	71.8	632	31	40	32	82%	0.50	0.06	64	0.09	0.25			7.03
7	95.1	729	19	32	27	86%	0.45	0.06	64	0.11	0.15			6.97
8	120.7	828	9	31	27	87%	0.47	0.05	69	0.19	0.20			6.91
9	144.8	931	3	26	21	82%	0.44	0.10	67	0.16	0.20			6.93
10	167.4	1,018	2	25	19	77%	0.43	0.06	64	0.15	0.25			7.20
11	190.9	1,171	1	19	15	79%	0.43	0.05	52	0.11	0.10			7.06
12	216.6	1,273	1	19	15	79%	0.44	0.09	56	0.13	0.15			6.81
13	217.1	1,371	1	18	13	75%	0.43	0.08	48	0.10	0.15			
14	217.5	1,471	1	na	na	na	na	na	na	na	0.10			6.90
15	218.0	1,571	na	13	9	76%	0.44	0.06	39	0.08	0.10			
16	218.5	1,673	na	na	na	na	na	na	na	na	na			7
17	219.0	1,774	na	na	na	na	na	na	na	na	0.35			
18	219.5	1,880	na	10	8	81%	0.39	0.07	32	0.04	0.10			6.92
19	219.9	1,974	na	na	na	na	na	na	na	na	0.15			
20	220.4	2,071	na	na	na	na	na	na	na	na	0.10			6.96
21	221.0	2,172	na	8	6	72%	0.41	0.07	30	0.05	0.15			6.90

Table S7. Push-pull data from the Br only injection. Compilation of the data collected during the Br only push-pull experiment, where 540 L of water from well I-1 was modified with 130 mg/L of Br and pushed it into well I-3. This injection was followed by another 80 L of unaltered water from I-1. After two days, the water was continuously withdrawn. Volume and Br concentrations are presented with the cumulative amount of Br removed.

Sample	Volume	Br	Cumulative Br
	L	mg/L	mg
Receiving well			
Source well			
Injection	540 +80	130	75.7
1	3	2.5	0.00
2	16	2.8	0.03
3	30	5.5	0.1
4	48	19.5	0.4
5	69	52.3	1.3
6	85	79.0	2.1
7	94	91.7	2.9
8	103	106.4	3.8
9	122	117.7	6.0
10	138	122.1	8.2
11	159	128.4	10.9
12	179	123.8	13.6
13	191	127.5	15.4
14	204	130.8	17.4
15	243	129.8	22.8
16	280	125.6	28.0
17	313	126.1	32.3
18	350	130.8	37.4
19	380	128.4	41.7
20	416	126.6	46.4
21	465	121.6	52.5
22	514	113.1	58.0
23	548	104.1	61.6
24	580	88.1	64.3
25	618	73.8	66.9
26	649	56.9	68.5
27	685	43.8	70.2
28	732	28.2	72.0
29	776	18.8	72.7
30	819	12.2	73.1
31	866	7.5	73.3
32	907	6.2	73.5

Table S8. Results of the As adsorption experiments on brown sediments. Equilibrium partitioning and capacity (K and S_{max}) were determined in the batch isotherm experiments. K was also estimated for a lower range of As concentrations (<3,000 µg/L). Using the S_{max} from the batch isotherms, K and the kinetic parameters (x_e, k_f and k_{diff}) were determined in the batch kinetic experiment. For the push-pull experiments, kinetic parameters were estimated using the range of Ks (30, 50 and 70) estimated from the batch experiments and suggest that only 2 to 5% of the adsorption sites were exposed. K from the push-pull experiments was also estimated using a x_e measured in similar aquifers ($x_e = 20\%$) and assuming single porosity (100%).

		Batch Isotherms						Batch Kinetic	
		Additions up to 32,000			Additions less than 3,000			AsIII	
		55m- AsIII	58m - AsIII	58m- AsV	55m- AsIII	58m - AsIII	58m- AsV	**One Site**	**Two Site**
K	L/kg	14.7	19.9	20.1	12.8	28.7	48.6	68	68
S_{max}	µg/kg		40,000	40,000	40,000*	40,000*	40,000*	40,000*	40,000*
x_f	%	--	--	--	--	--	--	100%*	23%
k_f	1/hr	--	--	--	--	--	--	0.05	0.3
k_{diff}	1/hr	--	--	--	--	--	--	--	0.006
r^2		0.97	0.99	0.98	0.82	0.84	1.00	0.85	0.99

--   parameter not needed
*   parameter set based on other experiment

|		Push Pull					
		AsV			AsIII		
		One Site	**Two Site**		**One Site**	**Two Site**	
			Set x_f	Set K		Set x_f	Set K
K	L/kg	1.8	5.1	50	0.5	1.7	12.8
S_{max}	µg/kg	40,000*	40,000*	40,000*	40,000*	40,000*	40,000*
x_f	%	100%	25%	3%	100%	25%	3%
k_f	1/hr	0.4	1.8	16.0	0.2	0.7	7.5
k_{diff}	1/hr	--	4.30E-03	3.38E-04	--	1.00E-03	3.00E-04
r^2		0.87	0.98	0.97	0.94	0.96	0.99

--   parameter not needed
*   parameter set based on other experiment

Table S9. Model results for one observation location and high-As area at approximately 160 m depth*. Time before breakthrough of 10% of initial [As] and normalize concentration at a time of 1,000 years are given for observation location shown in Fig. 3. Vulnerable area defined as percent of the high-As area with normalized [As] greater than 10% of initial [As] is given for 1,000 y and 5,000 y simulation times.

Pumping Scheme	Domestic Pumping Rate	K_d	Kh:Kv	Observation Location (Fig. 2)		Vulnerable Area (%) within High-As Area	
	[L/p-day]	[L/kg]		Years until C/C_0=0.1	C/C_0 at 1,000 y	1,000 y	5,000 y
Split	50	0	Base	526	0.79	56	70
Split	50	1.2	Base	>5,000	0	1	29
Split	50	12	Base	>5,000	0	0	0
Split	200	0	Base	143	1	84	85
Split	200	1.2	Base	1204	0.05	9	81
Split	200	12	Base	>5,000	0	0	2
Deep	50	0	Base	70	1	92	92
Deep	50	1.2	Base	570	0.36	63	92
Deep	50	12	Base	4950	0	4	41
Decreased Anisotrophy/ Increased Vertical Conductivity							
Split	50	1.2	1,000:1			11	57
Split	50	1.2	100:1			48	69

*The depth of the center of the uppermost finite-difference cell in the deep pumping zone is 162 m. In some areas, primarily outside of the high-As area, this depth is shallower due to thinning of basin sediments.
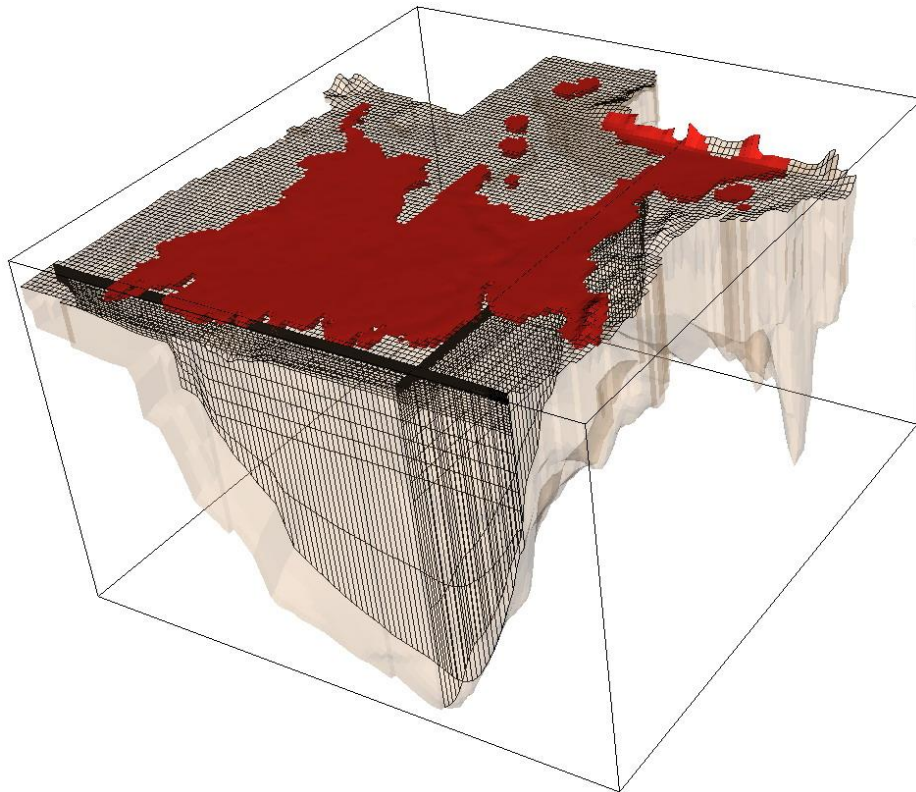
Figure S1. Model geometry, finite difference grid, and boundary and initial conditions for solute transport (red: C=1, no color: C=0). Vertical exaggeration is 100:1.
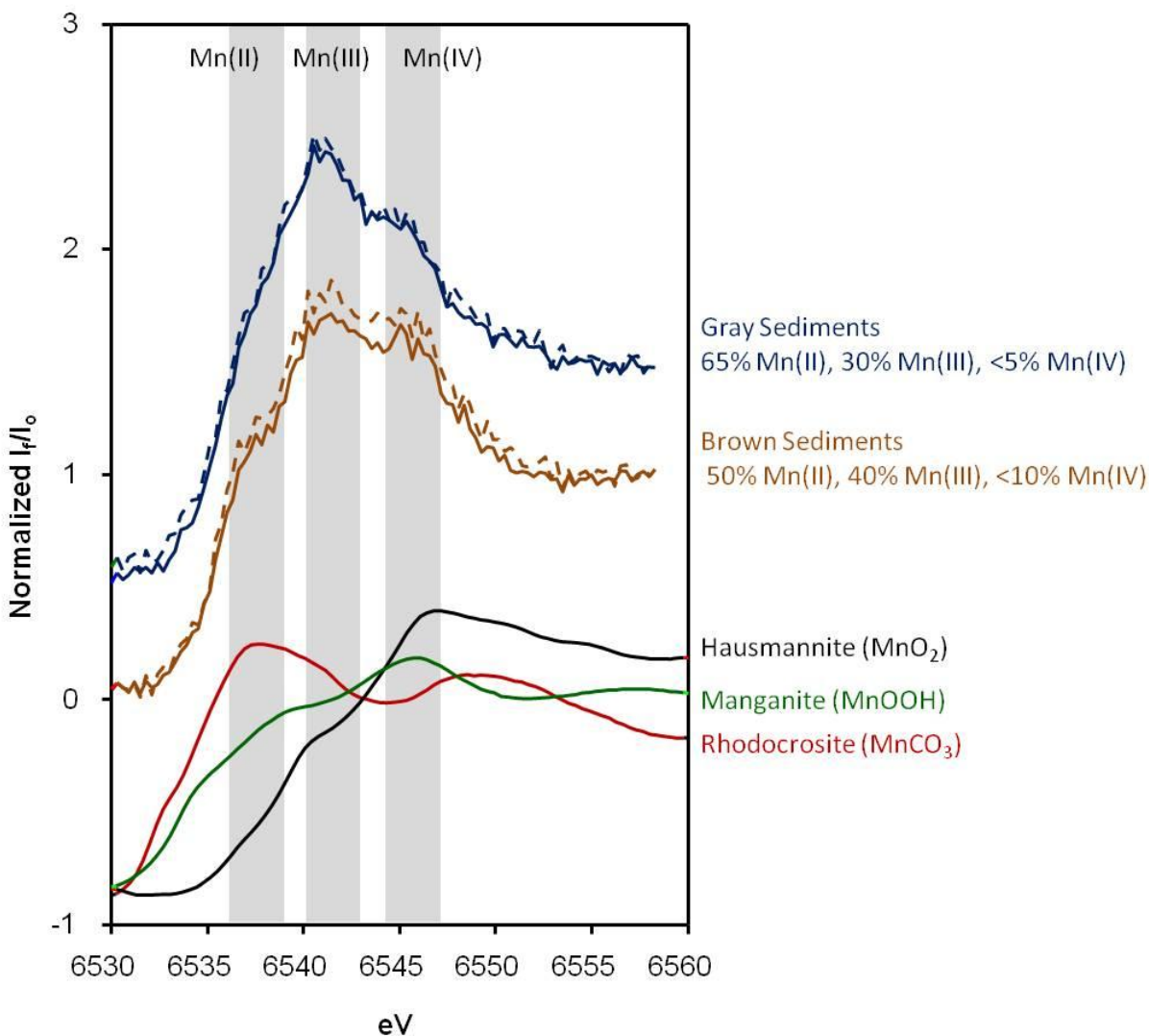
Figure S2. Mn speciation by X-ray absorption near edge spectroscopy (XANES). Measured spectra from the gray (40 m depth) and brown (58 m) sediments this site are shown along with three Mn reference minerals. Fits of the sediment spectra were produced by linear combination (dashed lines). Mn minerals in the sediments at both depths are predominately Mn(II) with a smaller contribution of Mn(III) minerals, while less than 10% of the Mn is present as Mn(IV).
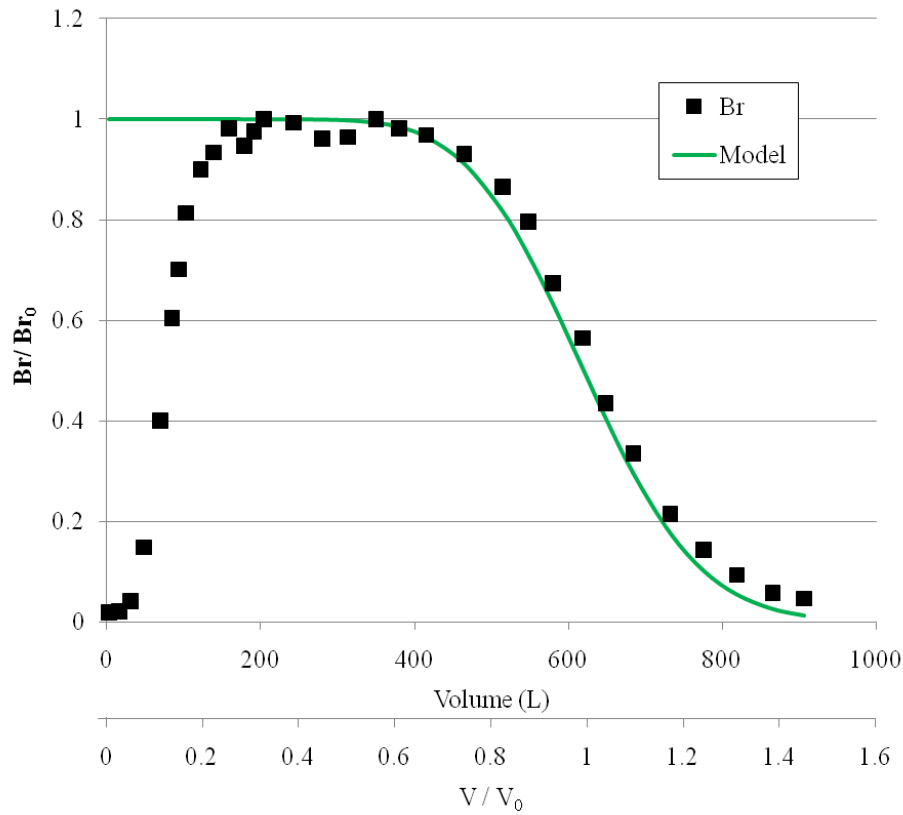
Figure S3. Br recovery over continuous pull with estimated disperstivity. Measured Br concnetrations from the tracer only push-pull were used to estimate aquifer disperstivity using the method described in Schroth, 2001. This test injected 540 L of water modified with 130 mg/L of Br followed by another 80 L of unaltered water. After two days, the water was continuously withdrawn. The model fit shown is with a disperstivity of 0.5 cm for the estimated 73 cm radius of influence for this push-pull test.
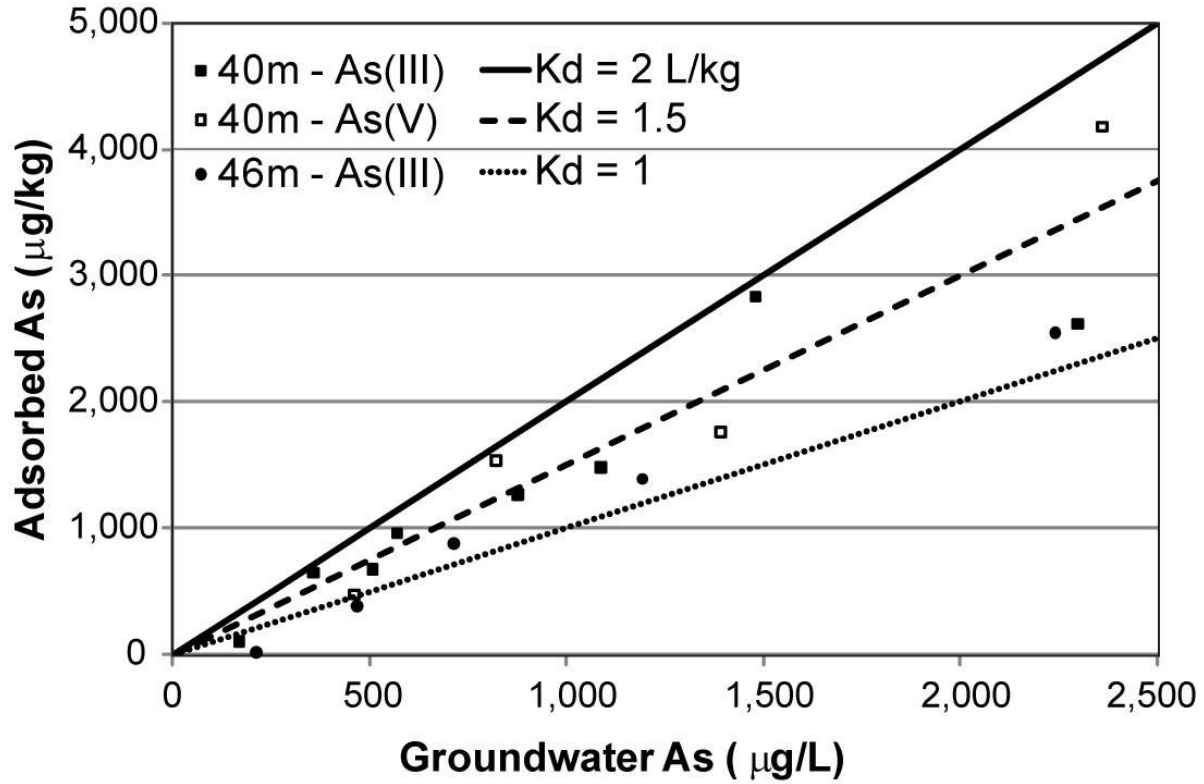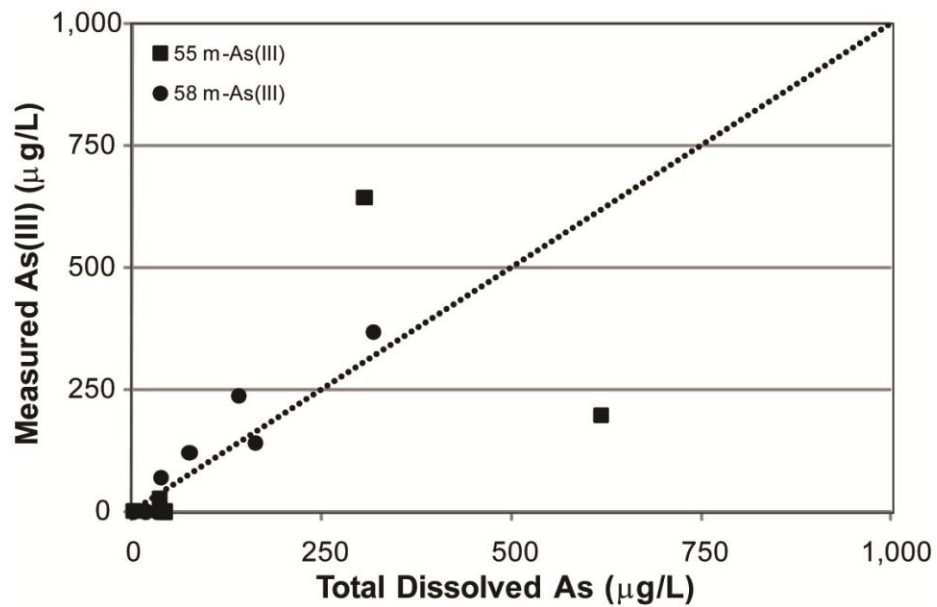
Figure S4. Batch isotherm experiments. Groundwater spiked with As(III) or As(V) was mixed with cuttings from the gray aquifers and sampled 145 hours later. Saturation was not reached on the gray sediments, therefore the partitioning coefficient, Kd, was estimated to be 1.5 L/kg.
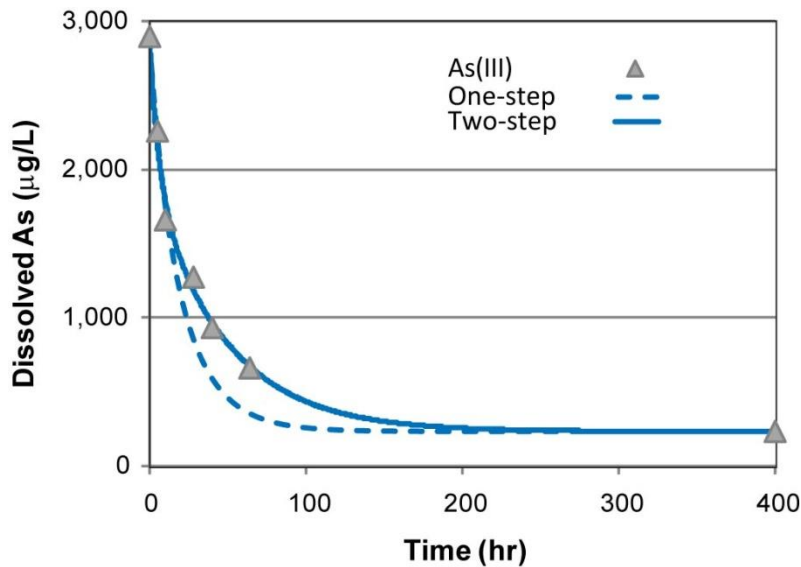

Figure S5. Batch kinetic results. Adsorption of spiked As(III) was observed over 400 hours on brown sediment collected at 58 m and had a K of 68 L/kg. Kinetic data was modeled using either the single or two-step models.
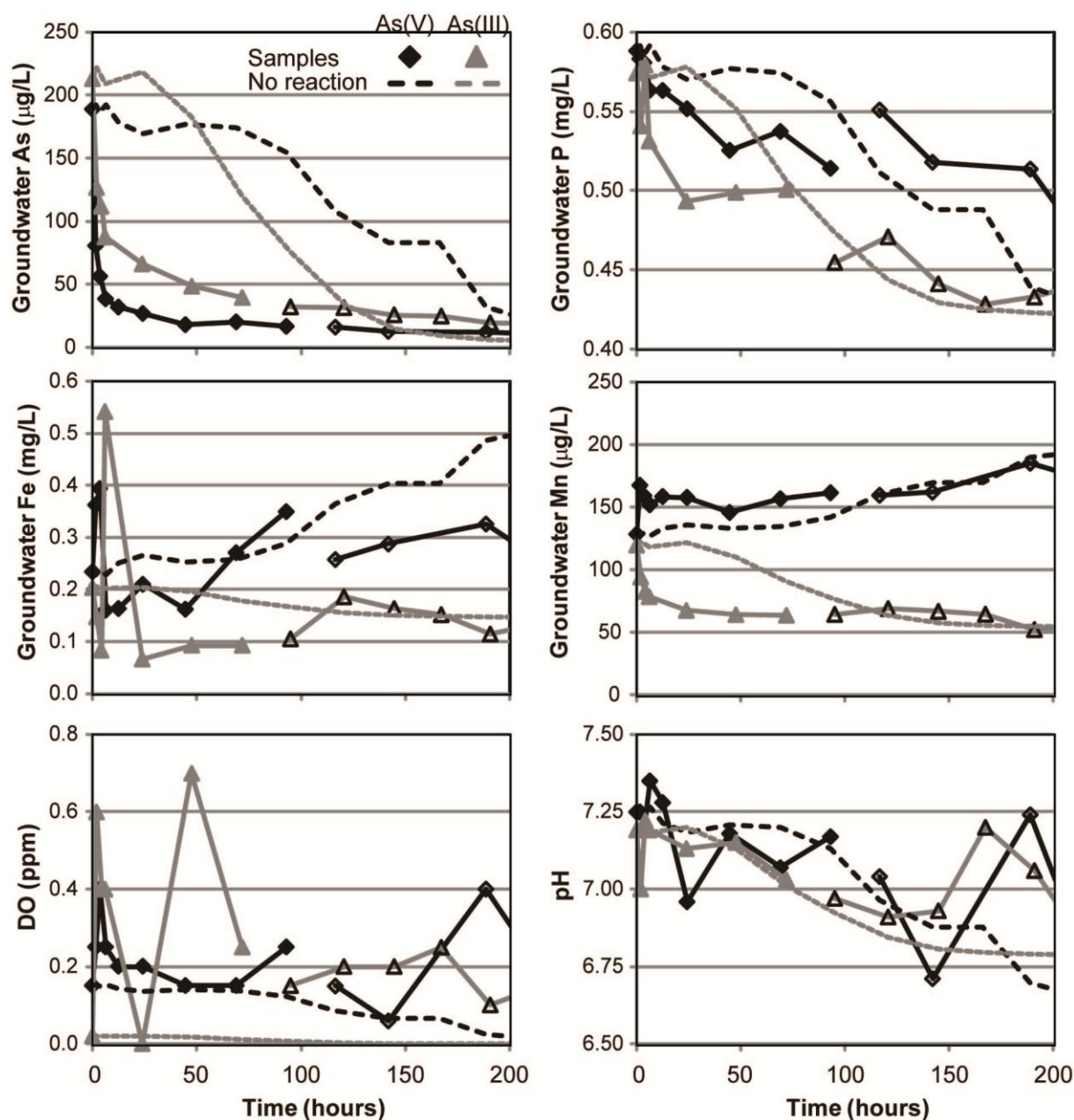
Figure S6. Push-pull results. Concentrations of As, P, Fe and Mn are shown as well as DO and pH. Results from the As(V) (black diamonds) and As(III) (gray triangles) push-pull tests are shown, with filled symbols indicating samples before significant Br dilution ([Br]/[Br]$_0$ > 85%). The dashed lines indicate the expected concentrations if no reaction had occurred and are based on the concentrations in the source and receiving wells and [Br].

Figure S7. Speciation of supernatant As in batch isotherm experiments. Groundwater As speciation was measured by voltammetry when the samples were collected. Results suggest that spiked As(III) remained as As(III) in solution; the dashed line indicates when total groundwater As is completely As(III).
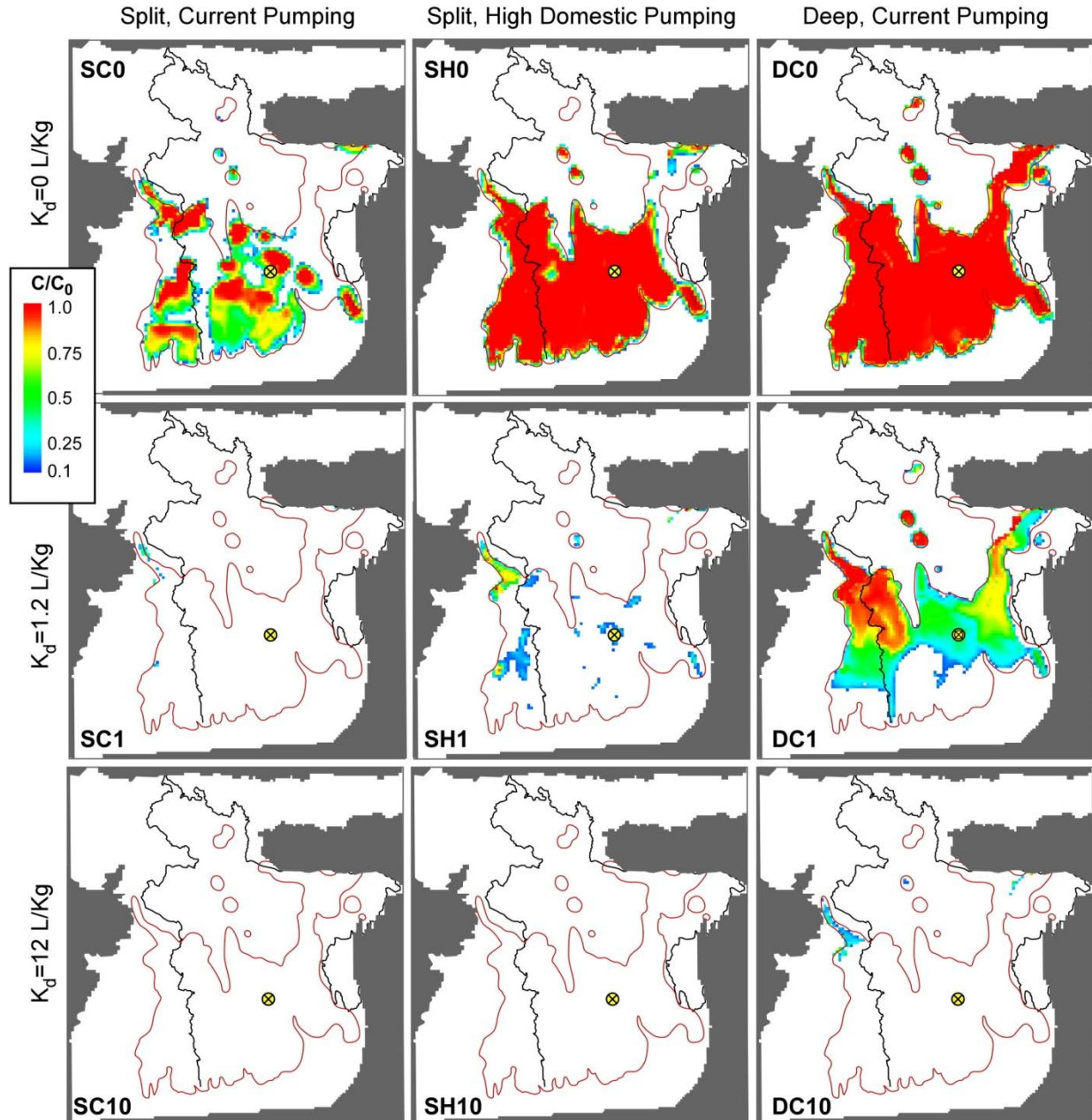
Figure S8. Areas of the deep low-As aquifer zones at risk of contamination, including simulations using $K_d = 12$ kg L^{-1}. Model boundary is enclosed in gray. Black line indicates the Bangladesh border and the red lines encircle the regions with high-As groundwater in the shallow aquifer zones (*2, 13*). The color scale indicates simulated [As] for $C/C_0 > 0.1$ after 1,000 yr at a depth of 162 m below ground surface. Modeled [As] is shown for the 3 water use scenarios (SC, SH and D) - current 'split' with shallow irrigation and deep domestic pumping at 50 L day^{-1} person^{-1} (SC), future 'split' with domestic use increased to 200 L/day-person (SH) and 'deep' pumping where both irrigation and current domestic use occurs in the deeper aquifer zone (DC) - and for no ($K_d = 0$ kg L^{-1}), low ($K_d = 1.2$ kg L^{-1}) and high retardation ($K_d = 12$ kg L^{-1}) for each scenario. The yellow dot indicates the location of plotted concentrations in Fig. 3.